

RESEARCH ARTICLE

Role of epithelial Na⁺ channels in endothelial function

Dongqing Guo¹, Shenghui Liang¹, Su Wang¹, Chengchun Tang², Bin Yao³, Wenhui Wan³, Hailing Zhang⁴, Hui Jiang⁵, Asif Ahmed⁶, Zhiren Zhang^{7,*} and Yuchun Gu^{1,*}

ABSTRACT

An increasing number of mechano-sensitive ion channels in endothelial cells have been identified in response to blood flow and hydrostatic pressure. However, how these channels respond to flow under different physiological and pathological conditions remains unknown. Our results show that epithelial Na⁺ channels (ENaCs) colocalize with hemeoxygenase-1 (HO-1) and hemeoxygenase-2 (HO-2) within the caveolae on the apical membrane of endothelial cells and are sensitive to stretch pressure and shear stress. ENaCs exhibited low levels of activity until their physiological environment was changed; in this case, the upregulation of HO-1, which in turn facilitated heme degradation and hence increased the carbon monoxide (CO) generation. CO potently increased the bioactivity of ENaCs, releasing the channel from inhibition. Endothelial cells responded to shear stress by increasing the Na⁺ influx rate. Elevation of intracellular Na⁺ concentration hampered the transportation of L-arginine, resulting in impaired nitric oxide (NO) generation. Our data suggest that ENaCs that are endogenous to human endothelial cells are mechano-sensitive. Persistent activation of ENaCs could inevitably lead to endothelium dysfunction and even vascular diseases such as atherosclerosis.

KEY WORDS: Mechanical stress, ENaC, Heme, NO, Endothelium dysfunction

INTRODUCTION

The endothelium is a thin layer of cells that line the interior surface of entire blood vessels, forming a physical barrier between circulating blood elements and underlying tissues. Endothelial cells are involved in many aspects of vascular biology, including the response to shear force, modulation of blood vessel tone and blood flow (Buchanan et al., 2014). There are many diverse responses of endothelial cells to hemodynamically related mechanical stress, ranging from ion channel activation to gene regulatory events (Davies et al., 1992).

Endothelial dysfunction is associated with most forms of cardiovascular disease, such as hypertension (Antonello et al., 2007), coronary artery diseases (Goel et al., 2007), peripheral artery diseases (Rhodes et al., 2015), diabetes (Prattichizzo et al., 2015) and chronic renal failure (Panizo et al., 2015). In hypertensive subjects with hyperaldosteronism, endothelium-dependent flow-mediated vasodilatation is impaired (Nishizaka et al., 2004).

Increased pulmonary blood flow in immature animals produces endothelial cell dysfunction with loss of endothelium-dependent vasodilatation before the onset of pulmonary vascular remodeling (Vitvitsky et al., 1998).

Ion channels expressed in endothelial cells are considered to mediate ‘short-term’ responses (in a range of seconds and minutes) to shear stress and subsequently affect cytoskeleton rearrangement and the synthesis and/or release of pro- and anticoagulants, growth factors and vasomotor regulators (Nilius and Droogmans, 2001). Epithelial Na⁺ channels (ENaCs) are expressed in a variety of endothelial cell types (Wang et al., 2009). These channels play a central role in controlling Na⁺ transport across epithelia and are thus of immense importance in all aspects of fluid clearance, as well as having numerous other functions. Administration of amiloride and benzamil, both antagonists of ENaCs, results in blockade of myogenic constriction of blood vessels (Jernigan and Drummond, 2005), suggesting a potential role of ENaCs in mediating vascular tone. Changes in plasma [Na⁺] are known to affect endothelial cell function, suggesting that ENaCs expressed in endothelial cells might contribute indirectly to the regulation of myogenic activity (Oberleithner et al., 2007). Additionally, aldosterone, a stimulator of ENaC activity and of the translocation of ENaCs in endothelial cell membranes (Oberleithner et al., 2006), has been shown to cause swelling of human umbilical vein endothelial cells (HUVECs) (Oberleithner et al., 2003), endothelium stiffening (Jeggle et al., 2013) and a decrease in NO production, resulting in endothelium dysfunction. Thus, a role for endothelial ENaCs in the control of vascular tone appears to be likely, but the nature of this role remains unclear. Additionally, inward rectified K⁺ (K_{ir}) channels have long been considered to be the principal shear-force-sensing ion channels in endothelial cells because K_{ir} channels are predominantly expressed in endothelial cells (Coleman et al., 2004) and the increase in K_{ir}-mediated K⁺ conductance is one of the most immediate cellular responses to shear force (Olesen et al., 1988). The primary cellular events following the activation of K_{ir} eventually lead to the generation and release of NO, causing the underlying smooth muscle cells to relax, leading to vasodilatation (Nilius et al., 1997). In our previous work, we showed that CO inhibits K_{ir} channels (Liang et al., 2014). Thus, it seems that CO as the product of hemeoxygenases is the signal to switch from K_{ir}- to ENaC-mediated control. However, whether ENaC can specifically contribute to flow sensing upon stimulation with inflammatory factors is unknown and is addressed in this study.

RESULTS

ENaCs are activated by fluid flow

We used whole-cell patch-clamping to record the Na⁺ currents (Fig. 1A). A flow rate of 5 ml/min (equivalent to 8.42 dyne) significantly augmented inward currents (Fig. 1B). This effect was completely reversed by benzamil (10 μM), an antagonist of ENaCs (Fig. 1B). This indicated that the shear-induced inward current was due to activation of ENaCs. The potentiation of inward current (normalized to control current) by fluid flow was directly dependent

¹Institute of Molecular Medicine, Peking University, Beijing, China, 100871. ²Department of Cardiology, The School of Medicine, South East University, Nanjing, China, 210009. ³Department of Cardiology, Nanjing General Hospital, Nanjing, China, 210000. ⁴Department of Pharmacology, Hebei Medical University, Shijiazhuang, China, 050017. ⁵Beijing Key Laboratory of Reproductive Endocrinology and Assisted Reproduction, Department of Urology, Peking University Third Hospital, Beijing, China, 100191. ⁶Aston Medical School, Aston University, Birmingham, B4 7ET, UK. ⁷Department of Pharmacology, 2nd affiliated hospital of Harbin Medical University, Harbin, China, 150000.

*Authors for correspondence (ycgu@pku.edu.cn; zhangzr@yahoo.com)

Received 18 January 2015; Accepted 21 November 2015

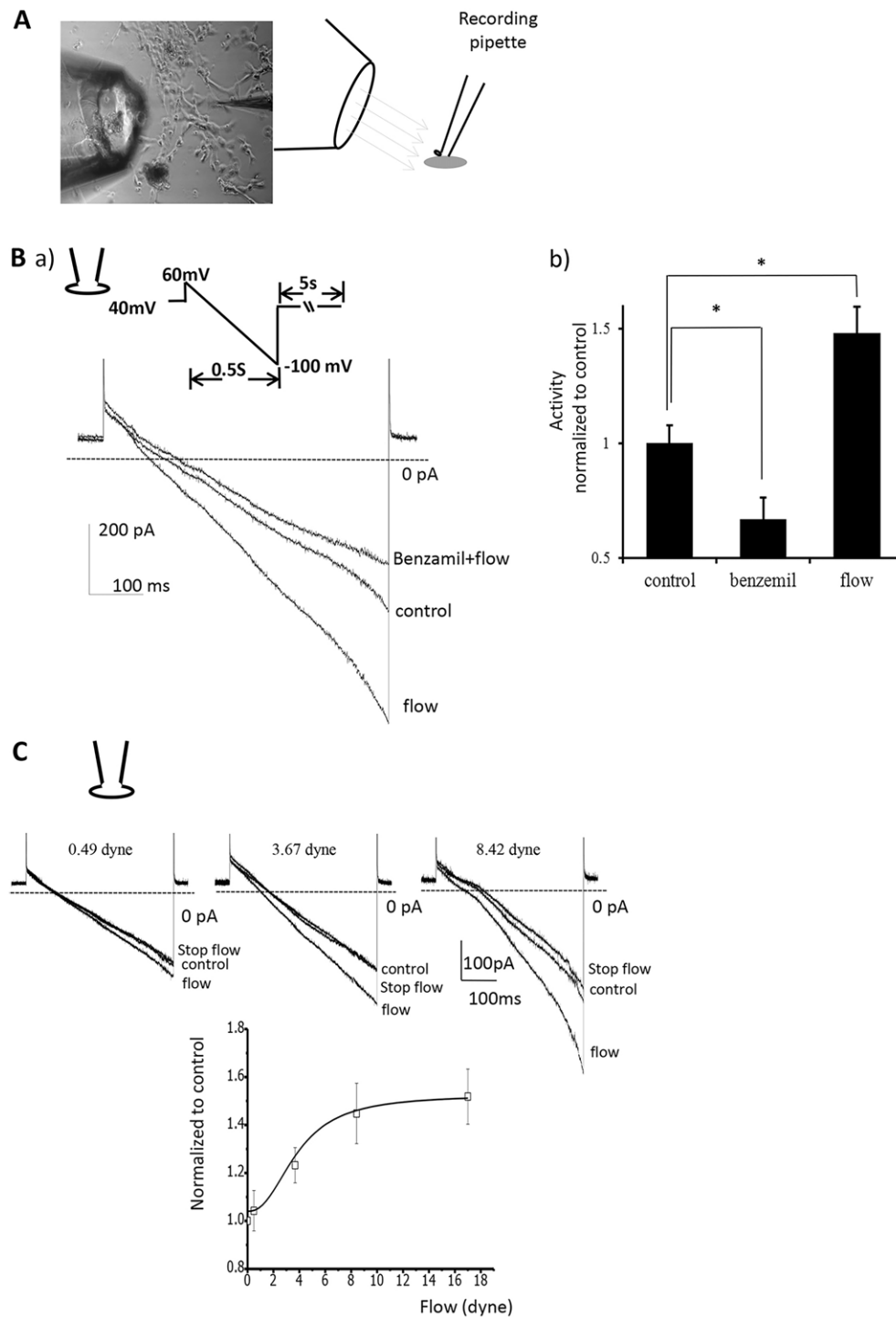


Fig. 1. Flow activated ENaCs. (A) In a conventional whole-cell recording setup, ENaC currents were elicited by using a voltage-ramp protocol. (B) In a conventional whole-cell recording setup, flow at a speed of 5 ml/min, which is equivalent to 8.42 dyne, significantly enhanced the inward currents mediated by ENaCs, which was reversed and blocked by benzamil (10 μ M). Each point represents the mean \pm s.e.m., * P <0.05 (Student's *t*-test), n =6–8. (C) Flow at speeds of 1, 3 and 5 ml/min, which are equivalent to 0.49, 3.67 and 8.42 dyne, respectively, substantially enhanced the inward currents mediated by ENaCs in a dose-dependent manner, which was reversed and blocked by stopping the flow. In the bottom graph, the x-axis represents shear stress acting on the cell membrane, and the y-axis represents the increased ratio of whole-cell current density carried by ENaCs. Each point represents the mean \pm s.e.m., n =4–5.

upon the amplitude of the flow-induced shear force, saturating at approximately 12 dyne (Fig. 1C).

ENaCs are activated by hydrostatic pressure and stretch

Positive pressure rather than suction was applied to the pipette, thus mimicking the effects of hydrostatic pressure on the apical surface of the membrane. Application of 10 mmHg increased activity of ENaCs almost 2.5-fold (Fig. 2A; P <0.05). Channel activity reached a maximum within 1 s of pressure application and decayed over a period of several seconds after release of pressure. Repeated stimulation elicited a similar response on every application

(Fig. 2A). Intriguingly, the flow-induced increase of channel-opening probability was also present in a cell-attached recording configuration where target channels had no direct contact with flow (Fig. 2B), suggesting that ENaCs can be, at least, activated by cell membrane tension and curvature.

Regulation of ENaCs by heme and CO

Using the inside-out configuration with a pipette voltage of +80 mV, we obtained traces that showed that different concentrations of heme could inhibit the activity of ENaCs (Fig. 3Aa), and the inhibitory effects were dose dependent

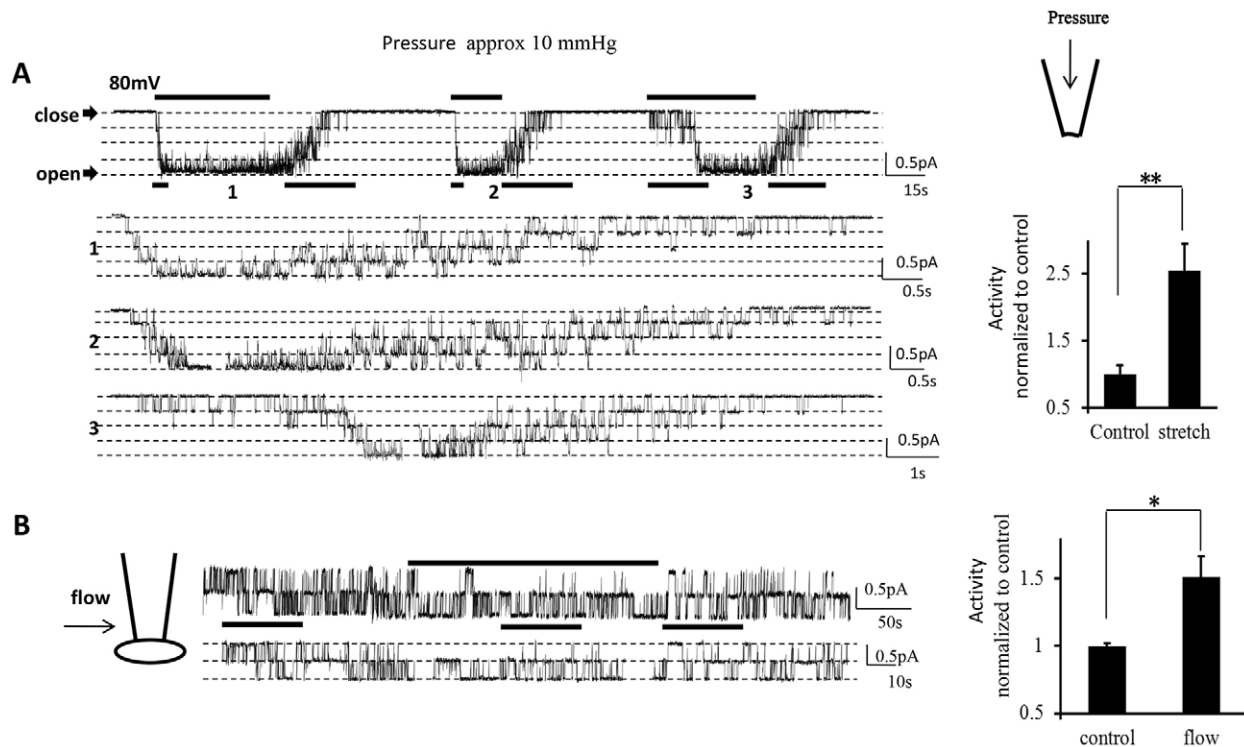


Fig. 2. Stretch-activated ENaCs. (A) In an inside-out recording, positive pressure (10 mmHg) applied through the patch pipette on the outside membrane of HUVECs activated ENaC currents in a repeatable manner. The pipette voltage was held at 80 mV. Stretch significantly increased ENaC activity by 1.5-fold. Each point represents the mean \pm s.e.m., $n=8$ (right side). (B) Indirect flow-mediated activation of ENaCs. In a cell-attached recording, flow significantly increased the open probability of ENaCs, suggesting the presence of an indirect mechanism. Application of pressure is shown by the black bars above the upper current trace. Selected parts of currents (marked by bars below the upper trace) are shown with an expanded time scale in the lower panel, correspondingly numbered. Each point represents the mean \pm s.e.m., $n=5$. * $P<0.05$, ** $P<0.01$, Student's t -test.

(Fig. 3B). However, addition of NADPH to heme-inhibited cells resulted in ENaC activity (Fig. 3Ab). This effect was reversed when HO-1 expression was knocked down (HO-1⁻) (Fig. 3Ac,Ad,C). CO, which is produced when cells are treated with heme plus NADPH, also activated ENaCs (data not shown).

ENaCs colocalize with caveolin-1, HO-1 and HO-2

Previous reports have demonstrated that ENaCs are present within lipid rafts (Sagi-Eisenberg et al., 1985). Accordingly, HUVECs were lysed, and the components of the membrane were separated by their density using a sucrose gradient. Twelve fractions were obtained; each fraction was precipitated and then immunoblotted with antibodies against the α -subunit of ENaC (also known as SCNN1A), caveolin-1, HO-1 and HO-2. Low-density membranes, which correspond to lipid rafts, were found near the top of the gradient in fractions 4 and 5, whereas non-raft markers were found at higher sucrose densities in fraction 8–12. Caveolin-1 was found in fractions 4 and 5. As well as ENaC α -subunit, HO-1 and HO-2 were detected in these fractions (Fig. 4A), suggesting that ENaC, HO-1 and HO-2 colocalize with caveolin-1.

TPA-induced increase in hemoxygenase expression enhances ENaC activity and shear sensitivity

Phorbol 12-myristate 13-acetate (TPA) is a potent tumor promoter and is also regarded as a common inflammatory factor (DeRiemer et al., 1985). TPA at a concentration of 100 ng/ml was added into the growth medium 24 h before experiments. Western blot analysis showed that HO-1 expression was significantly increased after 24 h

of stimulation with TPA, whereas the expression of caveolin-1, HO-2 and the α subunit of ENaC remained unchanged (Fig. 4B).

We then performed perforated whole-cell patch clamp analysis, a non-invasive method that monitors whole-cell currents while keeping the intracellular signaling molecules active. The results of perforated whole-cell patch clamping demonstrated a significant increase in Na⁺ conductance in response to a flow rate of 3 ml/min (equivalent to 3.67 dyne) in TPA-treated HUVECs, which was negligible in the results acquired from the non-TPA-treated HUVEC cells under the same conditions (Fig. 4C). Additionally, stimulation with TNF- α (25 ng/ml) exerted similar effects to those observed with TPA (data not shown). Taking all these data together, we conclude that the inflammatory factors could enhance ENaC activity and sensitivity to shear stress.

Increasing ENaC activity impedes cationic amino acid transporter activity and NO production

Increased ENaC activity leads to elevated intracellular Na⁺ concentration ([Na⁺]_i) in endothelial cells. We used whole-cell patch clamping to examine the corresponding currents that are induced by cationic amino acid transporter (CAT) proteins under different concentration of [Na⁺]_i. The inward currents evoked by extracellular L-arginine were significantly reversed, in a dose-dependent manner, by increasing [Na⁺]_i (Fig. 5A). The cellular availability of L-arginine is decided by the transport capacity of CAT proteins. Increased [Na⁺]_i, as we have demonstrated, reduces CAT activity and, in turn, impairs L-arginine entry. Therefore, ENaC-mediated shear-force sensing is likely to exert a reverse effect on endothelial cell function as it impairs endothelial-dependent NO

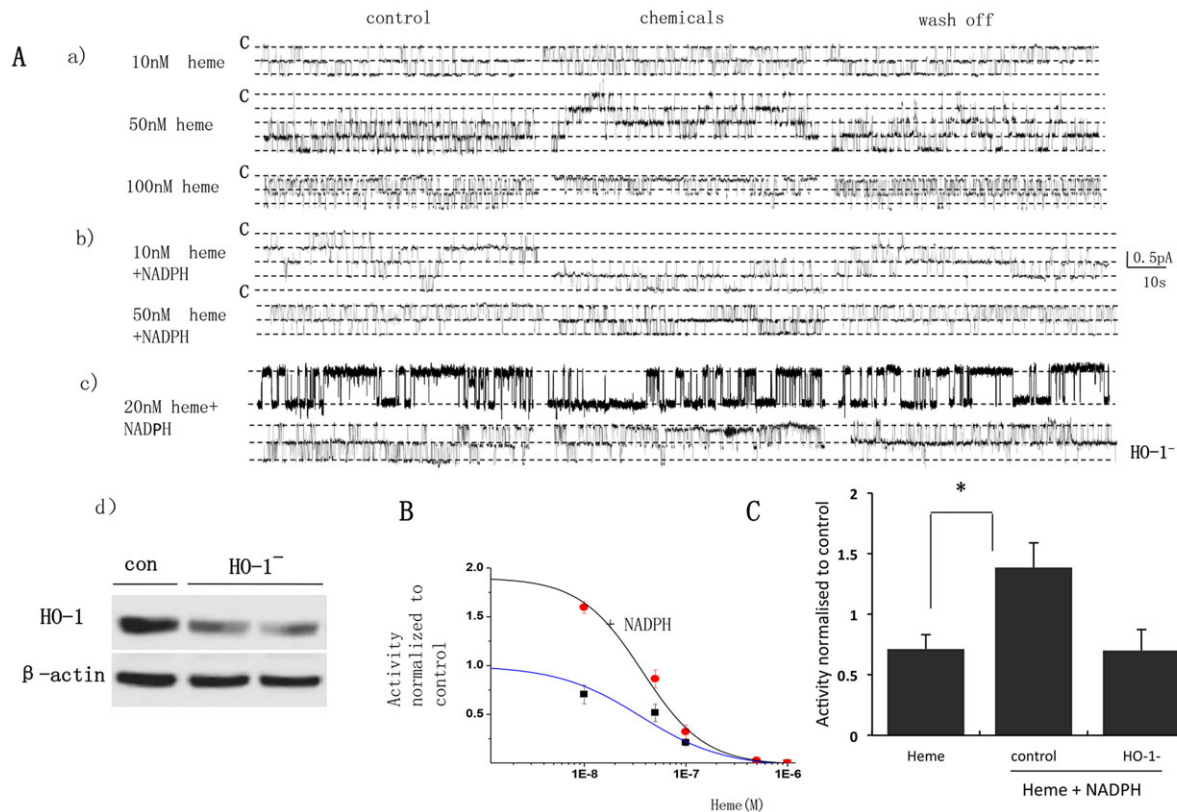


Fig. 3. Heme alone inhibits ENaCs, whereas heme plus NADPH activates ENaCs in HUVECs. (A) Traces were obtained using the inside-out configuration with a pipette voltage of +80 mV. (Aa) Different concentrations of heme inhibited ENaC activity. (Ab) Heme plus NADPH (1 μ M) activated ENaCs. (Ac) Heme plus NADPH (1 μ M) with knockdown of HO-1 (HO-1⁻) inhibited ENaCs. (Ad) Western blot analysis of HO-1 knockdown. Con, control. (B) Concentration-dependent effects of heme or heme plus NADPH on ENaC activity. Data were fitted with a sigmoidal dose-effect curve. The Hill coefficient is 0.99, based on the equation $Y = \text{minimum} + (\text{maximum} - \text{minimum}) / [1 + (X/X_0)^p]$. The blue line with black square symbols represents the effect of heme alone, and the black line with red circle symbols represents the effect of heme plus NADPH. Each point represents the mean \pm s.e.m., $n = 6-8$. (C) Statistical analysis of data shown in panel A. Heme (20 nM) significantly inhibited ENaC activity, whereas in presence of heme (20 nM) plus NADPH, ENaCs from HUVECs in which HO-1 (HO⁻) had been knocked down were inhibited. Each point represents the mean \pm s.e.m., $n = 10$. * $P < 0.05$, Student's t -test.

generation. We subjected HUVECs to shear force and found that NO production decreased owing to the resultant activation of ENaCs, whereas the ENaC antagonists benzamil and amiloride could reverse the process (Fig. 5B). Next, we isolated aortas from Wistar rats and explored the tension of aortic rings. The data shows that lipopolysaccharide (LPS; 20 μ g/ml) failed to dilate vessels owing to induced elevation of CO and consequently ENaC activation, whereas acetylcholine (10 μ M), which stimulates NO release, promoted vasodilatation (Fig. 5C).

DISCUSSION

We have identified the expression and the mechano-sensitivity of ENaCs in endothelial cells, determined the upregulation of HO-1 expression by inflammatory factors and validated the effects of the HO-1-mediated heme degradation pathway on ENaCs. By piecing all these findings together, we deduce that ENaCs are expressed on endothelial cells, and this expression provides a Na⁺ entry pathway and confers a mechanism by which cells can respond to mechanical stress. However, ENaC expression is suppressed until the physiological environment changes; in this case, the appearance of inflammation. Pro-inflammatory factors greatly upregulate the highly inducible protein HO-1, which in turn facilitates heme degradation and hence increases CO generation. CO potently increases the bioactivity of ENaCs, releasing the channels from inhibition, by contrast, CO exerts a

strong inhibitory effect on K_{ir} channels (Liang et al., 2014). This aspect of CO impact on endothelial cells can be therefore thought of as CO changing the responsibility of mechano-sensing from K_{ir} channels to ENaCs. Eventually, endothelial cells start to respond to shear stress by increasing the Na⁺ influx rate. Elevated [Na⁺]_i impairs L-arginine entry, resulting in impaired NO generation, whereas benzamil and amiloride, both antagonists of ENaCs, could rescue NO production. Thus, it is predicted that long-term ENaC hyper activation induced by chronic inflammation leads to decreased NO generation in endothelial cells and vasoconstriction.

Our results are consistent with many previous clinical reports (Nishizaka et al., 2004). For example, decreased L-arginine conversion to NO has been shown in hypertensive individuals after salt loading (Ni and Vaziri, 2001). Flow-mediated vasodilatation was significantly reduced in affected individuals compared to that in healthy control subjects (Pemp et al., 2009). Hemeoxygenases are the rate-limiting enzymes in heme catabolism, which leads to the generation of CO (Maines, 1997). Hemeoxygenases and their metabolic product, CO, have been implicated in the regulation of basal tone and blood pressure (Johnson et al., 1996). CO is a promising molecule with therapeutic potential in a number of vascular disorders owing to its cytoprotective and homeostatic properties (Dulak et al., 2008). CO inhibits sprouting angiogenesis and phosphorylation of

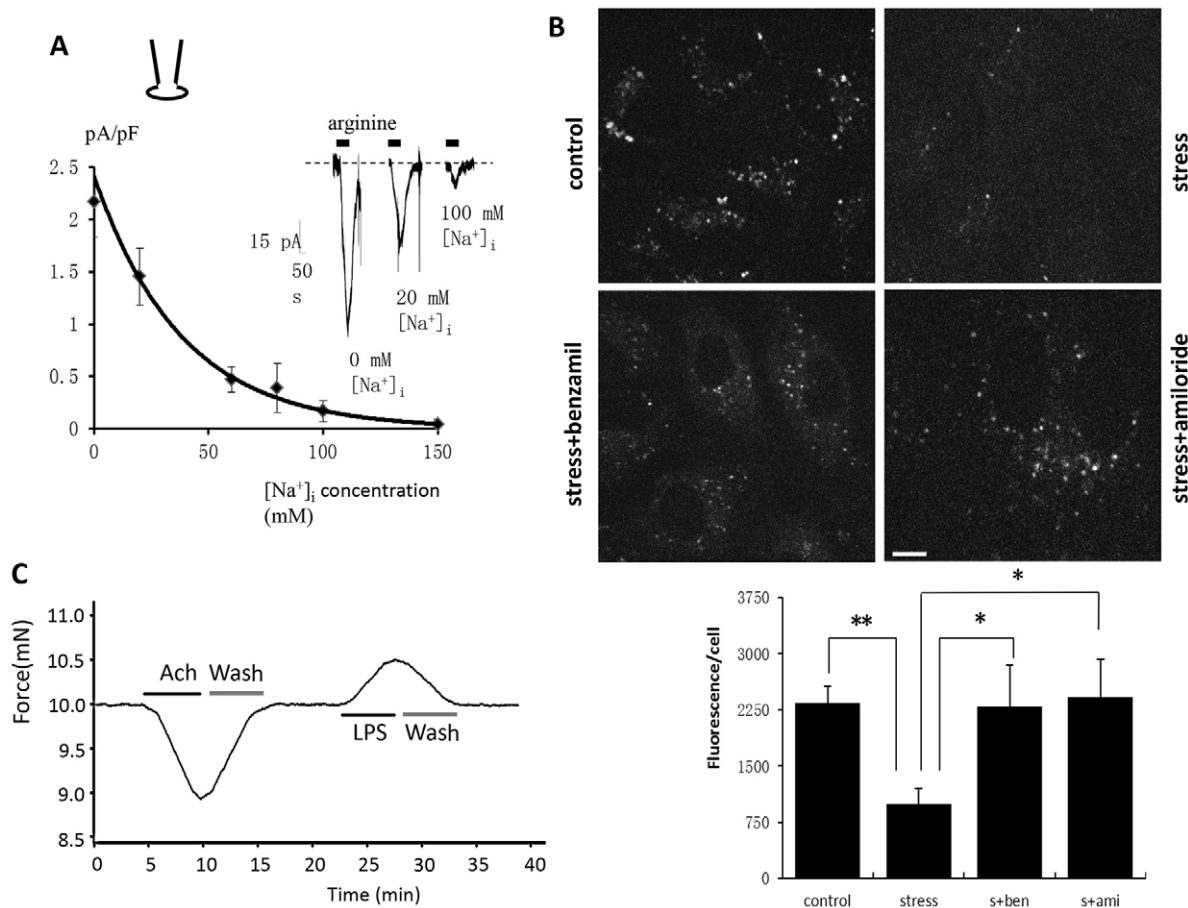


Fig. 5. An increase of ENaC activity impedes CAT activity and NO production. (A) An increase of $[Na^+]_i$ attenuated the activity of CAT proteins. The inward currents evoked by extracellular L-arginine were substantially reversed by an increase of $[Na^+]_i$ in a dose-dependent manner. Each point represents the mean \pm s.e.m., $n=4-6$. The curve was fitted using exponential decay (first order) on the equation $y=A1 \times \exp(-x/t1)+y0$. (B) Measurement of endothelial NO production using DAF-FM. Shear force decreased the NO production in HUVECs, and the ENaC antagonists benzamil and amiloride could reverse the process. Results represent the mean \pm s.e.m., $n=5$. Scale bar: 10 μ m. (C) The tension of aortic rings. Acetylcholine (ACh; 10 μ M), which stimulates NO release, promoted vasodilatation, whereas LPS (20 μ g/ml) failed to dilate vessels owing to induced elevation of CO and consequently ENaCs activation. s+ami, stress+amiloride; s+ben, stress+benzamil. * $P<0.05$, ** $P<0.01$, Student's *t*-test.

2015). Eventually, the initiation and progression of vascular diseases, such as atherosclerosis, is inevitable. Therefore, these results identify a pathological pathway that leads to chronic inflammation and to endothelial cell dysfunction, and that is characterized by decreased NO bioactivity, which is considered to be the first step towards vascular disease.

Our data identify that ENaCs that are endogenous to human endothelial cells are mechano-sensitive. Persistent activation of ENaCs induced by stimulation of inflammatory factors will inevitably lead to endothelium dysfunction and hypertension.

MATERIALS AND METHODS

Cell culture and chemicals

HUVECs were freshly isolated from human umbilical cord vein (ethics approval by the University Ethics Committee, Institute of Molecular Medicine, Peking University). HUVECs were grown in endothelial cell medium (Promocell) and maintained at 37°C under 5% CO₂. Cells were used within five passages.

All drugs were purchased from Sigma-Aldrich.

Electrophysiology recording

Single-channel recordings were performed as previously described (Liang et al., 2014). Briefly, a coverslip or insert on which HUVECs

had been cultured was transferred into a recording chamber mounted on a Nikon inverted microscope (Nikon TE 2000U). Patch pipettes of resistance 6 M Ω were fabricated from borosilicate glass capillaries (1.5 mm outside diameter, 0.86 mm inner diameter; Sutter) using a Sutter P97 pipette puller. Bath solution contained 110 mM NaCl, 4.5 mM KCl, 1 mM MgCl₂, 1 mM CaCl₂, 5 mM HEPES, 5 mM sodium HEPES, pH 7.2. Pipette solution contained 110 mM NaCl, 4.5 mM KCl, 0.1 mM EGTA, 5 mM HEPES, 5 mM sodium HEPES, pH 7.2. In the study of inward rectified K⁺ channels, bath solution contained 140 mM NaCl, 5.4 mM KCl, 1.8 mM CaCl₂, 1 mM MgCl₂, 5 mM HEPES, 10 mM glucose, pH 7.4 (adjusted with NaOH) and the pipette solution contained 100 mM potassium aspartate (Sigma-Aldrich), 30 mM KCl, 1 mM MgCl₂, 5 mM HEPES, 5 mM EGTA, 4 mM K₂-ATP, pH 7.3 (adjusted with KOH).

Single-channel currents were recorded with an Axon 200B amplifier connected to a PC running Axon clampex 9.0. The data were acquired at 20 kHz and low pass filtered at 5 kHz. During offline analysis, data were further filtered at 200 Hz. Single-channel events were listed and analyzed by using Pclampfit 9.0 (single channel search in analyze function). The 50% threshold cross method was utilized to determine valid channel openings. When multiple channel events were observed in a patch, the total number of functional channels (N) in the patch was determined by observing the number of peaks detected on all-points amplitude histograms. NP_o, the product of the number of channels was used to measure the channel activity within a patch. Initial, 3–4 min,

single-channel recordings were normally used as the control. The activity of ENaCs during application of chemicals was normalized to activity during the control period to assess the effects of chemicals on ENaC activity. In some cases, ENaC activity during the application of chemicals was also compared to that of ENaCs when chemicals were washed off. These data were used to confirm the effects of chemicals. Data are presented as means±s.e.m. Means were compared using Student's paired *t*-test. Statistical significance was set as <0.05.

Whole-cell recording was performed using pipettes of 6 MΩ resistance as detailed above. Bath saline was as described above but with the addition of 10 mM D-glucose. The pipette solution contained 40 mM KCl, 100K-gluconate, 1 mM MgCl₂, 1 mM CaCl₂, 0.1 mM EGTA, 4 mM Na₂ATP, 10 mM glucose, 10 mM HEPES and 2 mM GTP, and the pH was adjusted to 7.2 with KOH. For perforated patch whole-cell recording, the pipette solution was supplemented with 10–20 μg/ml amphotericin B. On the day of experiment, 0.1 g amphotericin B (Sigma-Aldrich) was dissolved in 0.1–0.5 ml DMSO to make a stock solution. 0.5 μl of this stock solution was added into 1 ml of pipette solution to make up the final pipette solution, giving a final amphotericin B concentration of 10–20 μg/ml. DMSO (vehicle for amphotericin B) at the same dilution was tested in control experiments, but no effect was observed.

Flow setup

Flow setup was performed as described previously by David E. Clapham with modifications (Oancea et al., 2006). A pipette with a wide opening in the range of 100–200 μm, which was connected to a syringe pump (Harvard Apparatus, Harvard), was placed within 160 μm of the cell of interest. When the whole-cell configuration was obtained, and the cell membrane potential was clamped at –100 mV, the pump was switched to generate a relative laminar flow over the cell of interest. The flow-induced shear force applied to the cell of interest was calculated according to the equation:

$$T = \frac{\rho V^2}{2} \times \frac{0.664}{\sqrt{R_x}}$$

where ρ is the density of water (1025 kg/m³), V is the fluid velocity [calculated using V=Q/A, where A=πd²/4 (d is the flow application pipette diameter) and Q is the flow rate generated by the syringe pump measured in m³/s]. R_x=V×X/μ, where X is the distance between pipette and cell; μ is the kinematic viscosity of the water (1.139×10⁻⁶ m²/s).

In our setup, d was approximately 120 μm and X approximately 160 μm. Accordingly, 1 ml/min of flow generated 0.49 dyne stress; 3 ml/min of flow was 3.67 dyne; 5 ml/min was 8.42 dyne; 8 ml/min was 17 dyne.

All data were obtained consistently. Whole-cell recording is a perfect way to monitor and evaluate the channel response to shear force. Therefore, it is used in the study of shear force response of ENaCs. However, cell-attached recording (single channel recording) is a good way, with less bias, to measure the response to hydrostatic pressure and was used to study the mechanical response of ENaCs. In these studies, 10 mmHg of hydrostatic pressure was applied.

Isolation of caveolae compartments, and western blotting

HUVECs were grown to confluence in 75-ml culture flasks and used for fractionation. The homogenate solution, in MBS buffer [25 mM 2-(N-morpholino)-ethanesulfonic acid (MES), pH 6.5, 0.15 M NaCl] containing 1% Triton X-100, was adjusted to 40% sucrose by the addition of 2 ml of 80% sucrose (in MBS) and was placed at the bottom of an ultracentrifuge tube. A 5–30% discontinuous sucrose gradient was formed above (4 ml of 5% sucrose, 4 ml of 30% sucrose, both in MBS lacking detergent) and centrifuged at 39,000 rpm for 18 h in an SW41 rotor (Beckman Instruments). A light-scattering band at the 5–30% sucrose interface was collected or fractionated into 12 sub-fractions.

Each fractionated protein sample was loaded and separated on a 10% Bis-Tris Gel. The membranes were then blocked with 5% non-fat dry milk, probed with appropriate primary antibodies, followed by incubation with horseradish peroxidase (HRP)-conjugated secondary antibodies at a dilution of 1:3000. Antibodies against the following proteins were used: ENaC

subunit α (Santa Cruz, sc-21012), HO-1 (Santa Cruz, sc-1796), HO-2 (Proteintech, 14817-1-AP) and caveolin-1 (Proteintech, 1644-1-AP).

Cell transfection

The HUVECs were seeded, and one day after seeding, were transfected with small interfering (si)RNA against HO-1 (GenePharma, Shanghai, China). In short, siRNA was mixed with PromoFectin-HUVECs (Promocell) in Opti-MEM reduced serum medium (Invitrogen) and incubated for 20 min at room temperature before being added to the apical side of the monolayer and further incubated for 5 h at 37°C. The transfection medium was then replaced with endothelial cell medium without antibiotics. Knockdown effects were examined by western blot analysis after 24 h.

The sequences targeted to silence HO-1 mRNA were 5'-GGGAAUUU-AUGCCAUGUAATT-3' (sense) and 5'-UUACAUGGCAUAAAUUCC-CTT-3' (antisense).

Measurement of endothelial NO production

HUVECs were stimulated with shear force for 8 h and treated with benzamil and amiloride. Then endothelial cells were incubated with 5 μM DAF-FM (Biyuntian, China) diacetate in Phenol-Red-free Dulbecco's modified Eagle's medium for 30 min at 37°C. The cells were washed gently with PBS three times; DAF fluorescence was observed by using ×60 oil objective lenses and analyzed with laser scanning confocal microscopy (Nikon).

Tension studies of aortic rings

Aorta tension studies were performed as previously described, with modifications (Faury et al., 1995). Male Wistar rats (250 g) were anesthetized with sodium pentobarbital (55 mg/kg, intraperitoneally) and killed by cervical dislocation. Rat aortas were quickly removed to a bath containing cold physiological salt solution (PSS) for dissection (154.7 mM NaCl, 5.4 mM KCl, 11.0 mM D-glucose, 2.5 mM CaCl₂, 6.0 mM Tris, pH 7.4). The distal aorta was dissected carefully to be free of surrounding tissue, cut as rings and mounted in a temperature-controlled myograph system (DanisMyo Technology A/S model: 610 M). The bath solution (PSS) was gassed with 100% O₂ at 37°C. Each ring was initially stretched to give an optimal pressure of 200 m/s², and the preparation was allowed to stabilize for 60 min. 10 μM of acetylcholine and 20 μg/ml LPS were used to perfuse. Tension data was relayed from the pressure transducers to a signal amplifier (600 series eight-channel amplifier, Gould Electronics). Data were acquired and analyzed with Pclamp software.

Statistical analysis

Student's *t*-test was used for the statistical analysis of all the independent experiments, with significance accepted at *P*<0.05. In the patch-clamping assays, data from one coverslip were averaged and are presented in the figures. The same experiment was repeated on different coverslips (*n*). Data are presented as mean±s.e.m., and statistical differences were assessed using Student's paired *t*-test. *P*<0.05 was considered significant.

Competing interests

The authors declare no competing or financial interests.

Author contributions

D.G., S.W. and Y.G. designed the experiments. D.G., S.L. and S.W. performed the experiments and analyzed the data. C.T., B.Y. and W.W. helped with the cell culture assays. H.Z. and H.J. helped with the tension studies of aortic rings. D.G. and Y.G. wrote the manuscript, and A.A., H.J. and Z.Z. revised the manuscript.

Funding

This work was supported by the research grants held by Y.G. from the 973 Project [grant numbers 2013CB531206 and 2012CB517803]; and the National Natural Science Foundation of China [grant numbers 81170236, 31127001 and 31221002].

References

Ahmad, S., Hewett, P. W., Fujisawa, T., Sissaoui, S., Cai, M., Gueron, G., Al-Ani, B., Cudmore, M., Ahmed, S. F., Wong, M. K. K. et al. (2015). Carbon monoxide inhibits sprouting angiogenesis and vascular endothelial growth factor receptor-2 phosphorylation. *Thromb. Haemost.* **113**, 329–337.

- Antonello, M., Montemurro, D., Bolognesi, M., Di Pascoli, M., Piva, A., Grego, F., Sticchi, D., Giuliani, L., Garbisa, S. and Rossi, G. P.** (2007). Prevention of hypertension, cardiovascular damage and endothelial dysfunction with green tea extracts. *Am. J. Hypertens.* **20**, 1321-1328.
- Buchanan, C. F., Verbridge, S. S., Vlachos, P. P. and Rylander, M. N.** (2014). Flow shear stress regulates endothelial barrier function and expression of angiogenic factors in a 3D microfluidic tumor vascular model. *Cell. Adh. Migr.* **8**, 517-524.
- Coleman, H. A., Tare, M. and Parkington, H. C.** (2004). Endothelial potassium channels, endothelium-dependent hyperpolarization and the regulation of vascular tone in health and disease. *Clin. Exp. Pharmacol. Physiol.* **31**, 641-649.
- Davies, P. F., Robotewskyj, A., Griem, M. L., Dull, R. O. and Polacek, D. C.** (1992). Hemodynamic forces and vascular cell communication in arteries. *Arch. Pathol. Lab. Med.* **116**, 1301-1306.
- DeRiemer, S. A., Strong, J. A., Albert, K. A., Greengard, P. and Kaczmarek, L. K.** (1985). Enhancement of calcium current in Aplysia neurones by phorbol ester and protein kinase C. *Nature* **313**, 313-316.
- Ding, Y., McCoubrey, W. K., Jr. and Maines, M. D.** (1999). Interaction of heme oxygenase-2 with nitric oxide donors. Is the oxygenase an intracellular 'sink' for NO? *Eur. J. Biochem.* **264**, 854-861.
- Dulak, J., Loboda, A. and Jozkowicz, A.** (2008). Effect of heme oxygenase-1 on vascular function and disease. *Curr. Opin. Lipidol.* **19**, 505-512.
- Faury, G., Ristori, M. T., Verdeti, J., Jacob, M. P. and Robert, L.** (1995). Effect of elastin peptides on vascular tone. *J. Vasc. Res.* **32**, 112-119.
- Goel, R., Majeed, F., Vogel, R., Corretti, M. C., Weir, M., Mangano, C., White, C., Plotnick, G. D. and Miller, M.** (2007). Exercise-induced hypertension, endothelial dysfunction, and coronary artery disease in a marathon runner. *Am. J. Cardiol.* **99**, 743-744.
- Hu, Q. S., Chen, Y. X., Huang, Q. S., Deng, B. Q., Xie, S. L., Wang, J. F. and Nie, R. Q.** (2015). Carbon monoxide releasing molecule accelerates reendothelialization after carotid artery balloon injury in rat. *Biomed. Environ. Sci.* **28**, 253-262.
- Jeggle, P., Callies, C., Tarjus, A., Fassot, C., Fels, J., Oberleithner, H., Jaisser, F. and Kusche-Vihrog, K.** (2013). Epithelial sodium channel stiffens the vascular endothelium in vitro and in Liddle mice. *Hypertension* **61**, 1053-1059.
- Jernigan, N. L. and Drummond, H. A.** (2005). Vascular ENaC proteins are required for renal myogenic constriction. *Am. J. Physiol. Renal Physiol.* **289**, F891-F901.
- Johnson, R. A., Lavesa, M., DeSeyn, K., Scholer, M. J. and Nasjletti, A.** (1996). Heme oxygenase substrates acutely lower blood pressure in hypertensive rats. *Am. J. Physiol.* **271**, H1132-H1138.
- Kim, H. P., Wang, X., Nakao, A., Kim, S. I., Murase, N., Choi, M. E., Ryter, S. W. and Choi, A. M. K.** (2005). Caveolin-1 expression by means of p38beta mitogen-activated protein kinase mediates the antiproliferative effect of carbon monoxide. *Proc. Natl. Acad. Sci. USA* **102**, 11319-11324.
- Leffler, C. W., Nasjletti, A., Yu, C., Johnson, R. A., Fedinec, A. L. and Walker, N.** (1999). Carbon monoxide and cerebral microvascular tone in newborn pigs. *Am. J. Physiol.* **276**, H1641-H1646.
- Leffler, C. W., Balabanova, L., Fedinec, A. L. and Parfenova, H.** (2005). Nitric oxide increases carbon monoxide production by piglet cerebral microvessels. *Am. J. Physiol. Heart Circ. Physiol.* **289**, H1442-H1447.
- Liang, S., Wang, Q., Zhang, W., Zhang, H., Tan, S., Ahmed, A. and Gu, Y.** (2014). Carbon monoxide inhibits inward rectifier potassium channels in cardiomyocytes. *Nat. Commun.* **5**, 4676.
- Maines, M. D.** (1997). The heme oxygenase system: a regulator of second messenger gases. *Annu. Rev. Pharmacol. Toxicol.* **37**, 517-554.
- Maulik, N., Engelman, D. T., Watanabe, M., Engelman, R. M. and Das, D. K.** (1996). Nitric oxide—a retrograde messenger for carbon monoxide signaling in ischemic heart. *Mol. Cell. Biochem.* **157**, 75-86.
- Mury, W. V., Brunini, T. M., Abrantes, D. C., Mendes, I. K., Campos, M. B., Mendes-Ribeiro, A. C. and Matsuura, C.** (2015). Hyperaggregability and impaired nitric oxide production in platelets from postmenopausal women. *Maturitas* **80**, 75-81.
- Ni, Z. and Vaziri, N. D.** (2001). Effect of salt loading on nitric oxide synthase expression in normotensive rats. *Am. J. Hypertens.* **14**, 155-163.
- Nilius, B. and Droogmans, G.** (2001). Ion channels and their functional role in vascular endothelium. *Physiol. Rev.* **81**, 1415-1459.
- Nilius, B., Viana, F. and Droogmans, G.** (1997). Ion channels in vascular endothelium. *Annu. Rev. Physiol.* **59**, 145-170.
- Nishizaka, M. K., Zaman, M. A., Green, S. A., Renfro, K. Y. and Calhoun, D. A.** (2004). Impaired endothelium-dependent flow-mediated vasodilation in hypertensive subjects with hyperaldosteronism. *Circulation* **109**, 2857-2861.
- Oancea, E., Wolfe, J. T. and Clapham, D. E.** (2006). Functional TRPM7 channels accumulate at the plasma membrane in response to fluid flow. *Circ. Res.* **98**, 245-253.
- Oberleithner, H., Schneider, S. W., Albermann, L., Hillebrand, U., Ludwig, T., Riethmuller, C., Shahin, V., Schafer, C. and Schillers, H.** (2003). Endothelial cell swelling by aldosterone. *J. Membr. Biol.* **196**, 163-172.
- Oberleithner, H., Riethmuller, C., Ludwig, T., Shahin, V., Stock, C., Schwab, A., Hausberg, M., Kusche, K. and Schillers, H.** (2006). Differential action of steroid hormones on human endothelium. *J. Cell Sci.* **119**, 1926-1932.
- Oberleithner, H., Riethmuller, C., Schillers, H., MacGregor, G. A., de Wardener, H. E. and Hausberg, M.** (2007). Plasma sodium stiffens vascular endothelium and reduces nitric oxide release. *Proc. Natl. Acad. Sci. USA* **104**, 16281-16286.
- Olesen, S.-P., Clapham, D. and Davies, P.** (1988). Haemodynamic shear stress activates a K⁺ current in vascular endothelial cells. *Nature* **331**, 168-170.
- Panizo, N., Rubio-Navarro, A., Amaro-Villalobos, J. M., Egido, J. and Moreno J. A.** (2015). Molecular Mechanisms and Novel Therapeutic Approaches to Rhabdomyolysis-Induced Acute Kidney Injury. *Kidney Blood Press. Res.* **40**, 520-532.
- Pemp, B., Weigert, G., Karl, K., Petzl, U., Wolzt, M., Schmetterer, L. and Garhofer, G.** (2009). Correlation of flicker-induced and flow-mediated vasodilatation in patients with endothelial dysfunction and healthy volunteers. *Diabetes Care* **32**, 1536-1541.
- Prattichizzo, F., Giuliani, A., Ceka, A., Rippon, M. R., Bonfigli, A. R., Testa, R., Procopio, A. D. and Olivieri, F.** (2015). Epigenetic mechanisms of endothelial dysfunction in type 2 diabetes. *Clin. Epigenet.* **7**, 56.
- Rhodes, C. J., Im, H., Cao, A., Hennigs, J. K., Wang, L., Sa, S., Chen, P.-I., Nickel, N. P., Miyagawa, K., Hopper, R. K. et al.** (2015). RNA sequencing analysis detection of a novel pathway of endothelial dysfunction in pulmonary arterial hypertension. *Am. J. Respir. Crit. Care Med.* **192**, 356-366.
- Sagi-Eisenberg, R., Lieman, H. and Pecht, I.** (1985). Protein kinase C regulation of the receptor-coupled calcium signal in histamine-secreting rat basophilic leukaemia cells. *Nature* **313**, 59-60.
- Vitvitsky, E. V., Griffin, J. P., Collins, M. H., Spray, T. L. and Gaynor, J. W.** (1998). Increased pulmonary blood flow produces endothelial cell dysfunction in neonatal swine. *Ann. Thorac. Surg.* **66**, 1372-1377.
- Wang, S., Meng, F., Mohan, S., Champaneri, B. and Gu, Y.** (2009). Functional ENaC channels expressed in endothelial cells: a new candidate for mediating shear force. *Microcirculation* **16**, 276-287.



Special Issue on 3D Cell Biology

Call for papers

Submission deadline: January 16th, 2016

Journal of Cell Science